Plasma Chemistry and Plasma Processing
https://doi.org/10.1007/s11090-018-9937-8

ORIGINAL PAPER

An Experimental Investigation of Cathode Spot Motion in a Magnetically Rotating Arc Plasma Generator at Atmospheric Pressure

Cheng Wang[1] · Jianqiao Li[1] · Zelong Zhang[1] · Lei Ye[1] · Weiluo Xia[2] · Weidong Xia[1]

Received: 4 July 2018 / Accepted: 11 October 2018

Abstract
Cathode spots present complex forms in magnetically rotating arc plasma generators due to the coupling effect of the plasma flow and electromagnetic fields. In this paper, a magnetically rotating arc plasma generator is built to study cathode spot motion at atmospheric pressure. Cathode spot configuration is observed and discussed for different magnetic fields, arc currents, gas flow rates and cathode lengths. Results show that cathode spots with a slow rotation speed (less than 1 Hz) and different rotation directions occur on the cathode end. For a low magnetic field, low arc current, high gas flow, short cathode rod, the rotation direction of the cathode spot is consistent with the arc column rotation. With an increase in the magnetic field, increase in the arc current, decrease in gas flow, or increase in the cathode rod length, the rotation speed declines, and the cathode spot can move in a reversed direction (i.e., against the arc column rotation). The cathode spot area also appears to expand gradually when the spot motion shifts from the normal direction to the reversed direction, resulting in less cathode erosion at the reversed motion. Further analysis indicates that the cathode spot motion is similar to the retrograde movement that occurs in a vacuum arc with an external magnetic field. The rotation of cathode spot may thus be induced by the radial component of the magnetic field. The cathode spot area that affects the self-magnetic field in the cathode spot is potentially a direct determinant of spot motion.

Keywords Cathode spot motion · Magnetically rotating arc plasma · Graphite cathode · Rotation of cathode spot · Reversed movement

✉ Weidong Xia
xiawd@ustc.edu.cn

[1] Department of Thermal Science and Energy Engineering, University of Science and Technology, Hefei 230027, China

[2] Hefei Institutes of Physical Science, Chinese Academy of Sciences, Hefei 230031, China

Published online: 25 October 2018

Introduction

Arc plasma is widely used in industrial applications owing to its high temperature, high enthalpy, and high chemical activity [1, 2]. The magnetically rotating arc plasma generator is a common form of plasma equipment. Induced by the axial magnetic field, the arc between the concentric electrodes rotates rapidly around the axis. Many experiments have confirmed that the rotating arc can increases the arc plasma volume [3, 4], improves the uniformity of the plasma parameters [4, 5], and decreases the electrode erosion [6–8]; thus, this arc was applied in many fields such as diamond films deposition [9, 10], gas synthesis [11, 12], aerosol analysis [13], and nano-sized materials preparation [14, 15].

Cathode spot motion plays an important role in arc discharge because it affects the configuration of the arc plasma and determines the electrode erosion rate. Compared with common plasma generators, cathode spot motion in a magnetically rotating arc plasma generator is more complicated due to strong plasma flow, substantial heating effect to the cathode, and complex magnetic disturbances in the cathode spot. In earlier research, high-speed retrograde rotation (i.e., against the Lorenz/Ampere direction) of the cathode spot was observed in magnetically rotating arc plasma generators under low pressure [16–18]. Generally, with a reduction in pressure, the rotation direction of the cathode spot changes from the Lorenz direction to the retrograde direction, while the arc column and anode spot moves constantly in the Lorenz direction. Such retrograde motion has been found to depend heavily on the arc current, gap length, gas pressure, electrode materials, and other factors. Numerous hypotheses were proposed to explain this phenomenon, such as pure surface effects, magneto-hydrodynamic instabilities, movement of ions and electrons, asymmetric magnetic pressure distribution and so on [19–27]; however, no explanation has been unanimously accepted. Additionally, retrograde motion seems to occur only with cold-cathode arcs [19].

At atmospheric pressure, cathode spot motion in magnetically rotating arc plasma generators is quite different because the hot cathode spot (thermionic emission) is dominant. The cathode spot usually moves quickly in the Lorenz/Ampere direction in accordance with the arc column and anode spot [8, 28, 29]. Recently, Xia et al. [30–34] observed the constricted mode and diffuse mode of the cathode spot in a magnetically rotating arc plasma generator, and a coupled sheath model was developed to predict the cathode spot mode transition. Moreover, the multi-spot mode, which is distributed discretely on the lanthanum tungsten/graphite cathode end, has been suggested in the literature [5, 14, 35–38]. Experimental and simulation analyses have revealed cathode temperature and arc configuration to be potential primary drivers behind cathode spot motion.

A slow-speed rotation of the cathode spot on the cathode end was also noticed in refs [14, 35, 37]. On the graphite cathode end, Xia et al. [35] discovered that the cathode spot rotated around the axis at a frequency of approximately a few Hertz, much lower than that of the arc column and anode spot. Due to the intense radiation emitted from the cathode spot, cathode spot movement caused low-frequency fluctuations in radiation. In addition, the speed difference between the cathode spot and arc column could induce large-scale arc shunting between the arc column and cathode end, resulting in highly unstable arc voltage [36]. Mihovsky et al. [14, 37] also found the rotation speed of the cathode spot on the graphite cathode end to be significantly lower than that of the arc column, but the spot movement only began at higher arc currents and a higher

magnetic field. Experimental findings regarding slow-speed rotation of cathode spots are so scarce that an understanding of this phenomenon remains elusive; however, spot motion can potentially affect applications involving the plasma generator.

A magnetically rotating arc plasma generator was constructed in this paper to study the slow-speed rotation of cathode spots. The arc operated on the graphite cathode at atmospheric pressure. The configuration of the cathode spot was obtained by a high-speed charge-coupled device (CCD) camera. Effects of the magnetic field, arc current, gas flow and cathode length on cathode spot motion are analyzed, and an explanation for cathode spot motion is proposed.

Experimental Setup

The experimental setup is shown in Fig. 1, primarily composed of a magnetically rotating arc plasma generator, two DC power sources, a gas supply unit, and a measurement system. The plasma generator consists of a hollow cylindrical anode (graphite; 200 mm in length and 20 mm in inner diameter), a concentric graphite cathode (50, 80, and 110 mm in length and 8 mm in diameter), and a magnetic coil surrounding the anode. In the experiment, the cathode was bolted by a water-cooling and moveable holder, and the cathode end was always approximately 50 mm in front of the anode exit by adjusting the moveable holder. The magnetic coil was connected to a DC power source. By controlling the currents, the axial magnetic field, induced by the magnetic coil, could be adjusted continuously within a range of 0–0.15 T. The gas inlet was distributed uniformly on the cathode flange. Argon gas was injected axially into the generator through the gas inlet. A modulated 0–200 V DC power supply (IGBT source with current fluctuation < 10% and conversion efficiency > 90%) was used for the arc plasma generator. A high-speed CCD

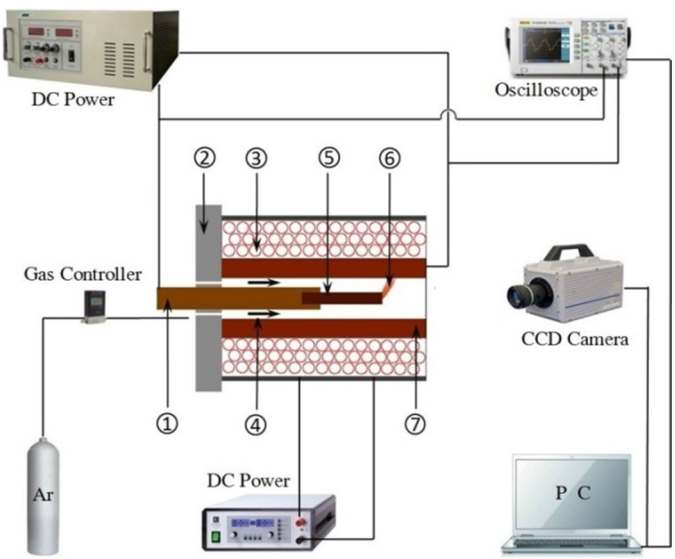

Fig. 1 Schematic diagram of the arc plasma device and experimental setup. ① cathode holder, ② gas inlet flange, ③ magnetic coil, ④ gas inlet, ⑤ cathode, ⑥ arc, ⑦ anode

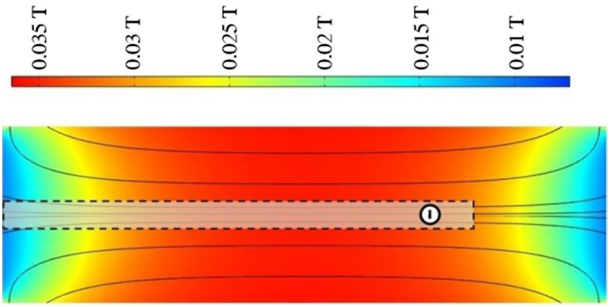

Fig. 2 Magnetic field flux lines in the anode simulated using COMSOL Multiphysics software, 10,000 amp-turns

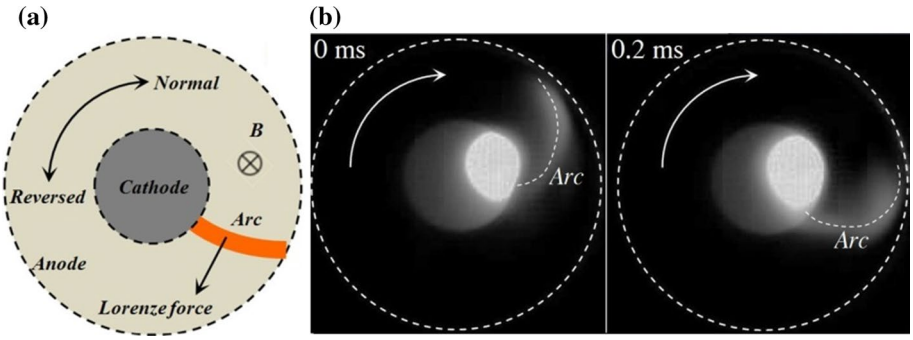

Fig. 3 Arc motion in the plasma reactor: **a** diagrammatic sketch, **b** CCD images of arc plasma (I = 80 A, B = 0.045 T, G = 25 slm, L = 80 mm, 2 μs shutter, 5000 fps)

camera (Photron, FASTCAM SA5 1000K-M3; 256 × 256 pixels, 256 gray levels, maximum 1,000,000 frames per second [fps]) was placed in front of the generator to capture images of the cathode arc spots. An oscilloscope (MDO3000; Tektronix) was used to acquire arc voltage signals and arc currents by a voltage divider. To observe the cathode spot more clearly, a narrowband filter (centered at 416 nm, Ar-I line) was placed in the camera lens to reduce strong radiation from the graphite cathode. All experiments were carried out at atmospheric pressure.

Magnetic field flux lines in the anode were simulated by COMSOL Multiphysics software, as shown in Fig. 2. The magnetic field flux lines in the cathode end were essentially parallel to the cathode axis, but a radial component existed; the radial component of magnetic flux density was approximately 5–10%. In this experiment, the magnetic field in the anode was recorded by a Gauss Meter (HT208; China). For restrictions in the experimental conditions, the magnetic field in the following sections refers to the axial component at the cathode end.

Figure 3 exhibits a typical arc motion in the magnetically rotating arc plasma generator. The arc is plotted by dotted white lines, so the arc motion can be seen more clearly. In Fig. 3b, the dashed outline represents the inner wall of the anode, and the cathode is located at the center of the cross-section. A luminous cathode spot appeared on the cathode end close to the cathode edge. The brightness of the arc column between the cathode and anode was much lower than that of the cathode spot due to the strong radiation emitted from the cathode spot. Driven by the Lorentz force, the arc column rotated clockwise

around the cathode at a speed of approximately 400 rounds per second (r/s). The cathode spot in the thermionic cathode often moved along with the arc column at atmospheric pressure; therefore, the clockwise direction was considered the normal direction whereas the counter-clockwise direction was considered reversed one, as shown in Fig. 3a.

The cathode spot area approached a circle as shown in Fig. 4, which also displays a typical intensity profile along the line crossing the cathode spot center. The cathode outline is denoted by a white dotted line. The radiation emitted from the cathode spot was so strong that it was difficult to obtain an accurate measurement of the cathode spot diameter. In this paper, the edge of the cathode spot is defined as the point where the intensity is saturated on the cathode end, as indicated in Fig. 4. The saturated region of radiation intensity exhibited a remarkable difference under different shutter times, and the shutter time was fixed at 0.5 μs when measuring the cathode spot diameter. The cathode spot diameter is a qualitative result; the measurement does not represent the physical diameter.

Results and Discussion

Magnetic Field

Figure 5 presents successive CCD images of cathode spots under different magnetic fields. To observe the cathode outline, the shutter time for each group was different. The arrowhead in these pictures represents the rotation direction of the cathode spot. In these pictures, the arc column rotated clockwise around the cathode at a speed of several hundred rounds per second, as shown in Fig. 3b. In a low magnetic field (0.03 T), the cathode spot moved in the normal direction as shown in Fig. 5a. After 5 min of counting, the rotation speed of the cathode spot was approximately 20 rounds per min (r/min). The rotation speed of the cathode spot was much lower than that of the arc column. When the magnetic field increased to 0.045 T, a distinct change occurred in the rotation direction of the cathode

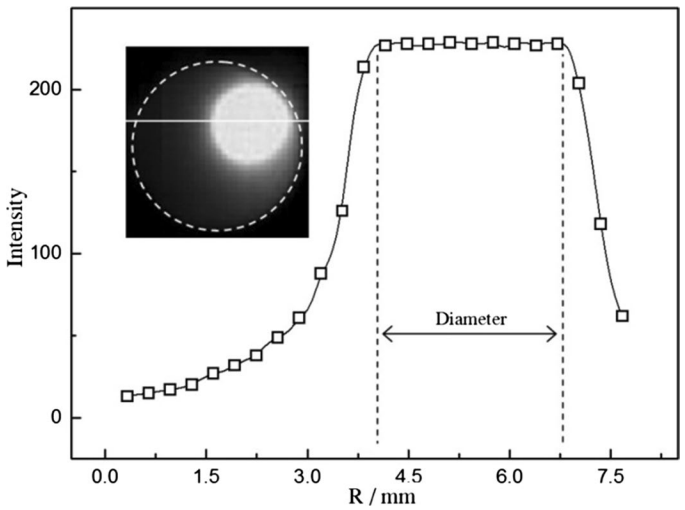

Fig. 4 CCD image of cathode spot and the estimation of cathode spot diameter (I = 80 A, B = 0.045 T, G = 25 slm, L = 80 mm, 0.5 μs shutter, approximately 3 mm diameter)

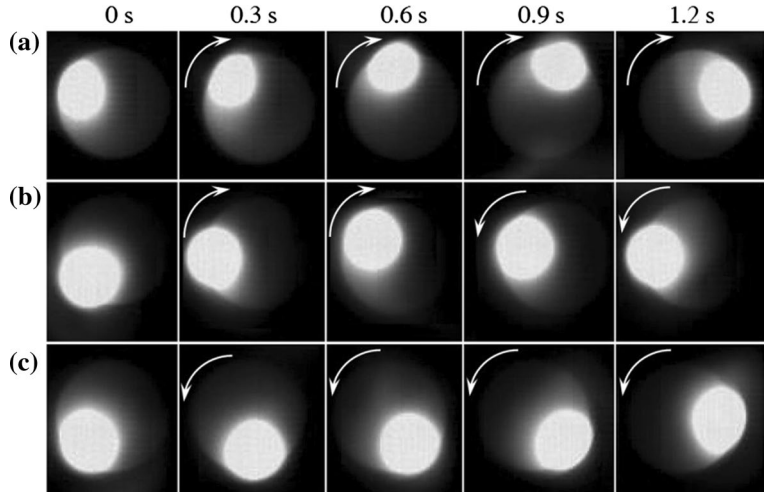

Fig. 5 Successive CCD images of cathode spots under different magnetic field (I = 80 A, G = 25 slm, L = 80 mm): **a** B = 0.03 T, 1 μs shutter; **b** B = 0.045 T, 1 μs shutter; **c** B = 0.075 T, 0.5 μs shutter

spot. As indicated in Fig. 5b, the cathode spot continued moving in the normal direction from 0 to 0.6 s whereas reversed movement took place from 0.6 to 1.2 s. The rotation speed of the cathode spot was less than 4 r/min after 5 min of counting because of the cumulative effect of normal and reversed movement. When the magnetic field increased to 0.075 T, the cathode spot moved in the reversed direction completely, as shown in Fig. 5c. As determined by statistical analysis, the rotation speed of the cathode spot was approximately 10 r/min.

Figure 6 exhibits typical CCD images of cathode spots under different magnetic fields. The shutter time was fixed at 0.5 μs so the configuration of cathode spots under different magnetic fields could be distinguished clearly. The rotation speed and cathode spot diameter corresponding to the CCD images in Fig. 6 are plotted in Fig. 7. At a low magnetic field (0.03 T), the cathode spot was quite small (approximately 2.5 mm) with a fast rotation speed in the normal direction (approximately 20 r/min). However, the brightness of the whole cathode end was so low that the cathode outline could not be observed clearly. With an increase in the magnetic field, the cathode spot diameter expanded gradually, increasing from 2.5 mm at 0.03 T to 4.5 mm at 0.135 T. The brightness of the whole cathode end was also enhanced by an increase in the magnetic field, which can be confirmed by the

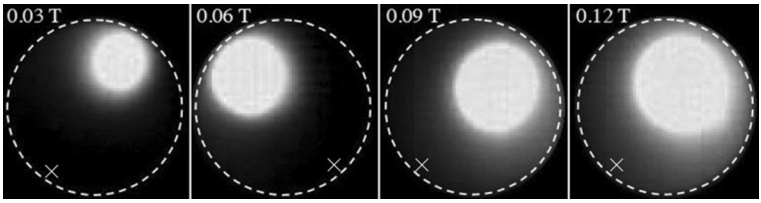

Fig. 6 CCD images of cathode spots under different magnetic fields (I = 80 A, G = 25 slm, L = 80 mm, 0.5 μs shutter, gray value at the edge of the cathode end: 7, 9, 16, 28, respectively)

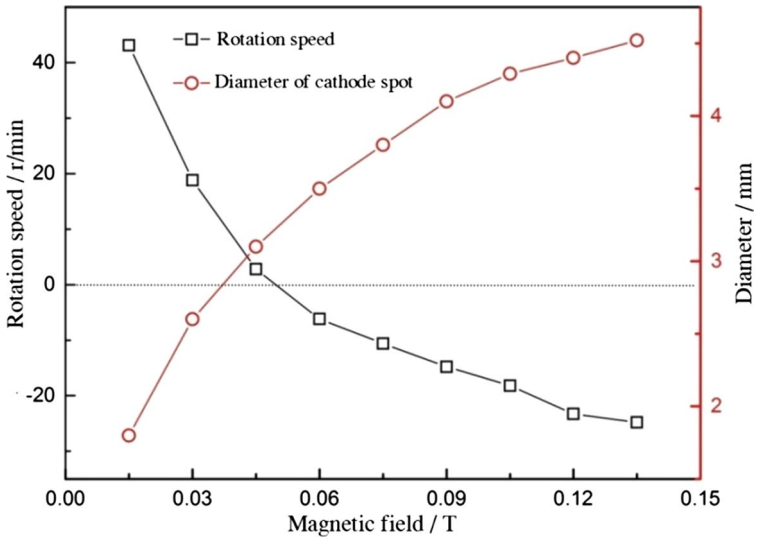

Fig. 7 Rotation speed and cathode spot diameter under different magnetic fields (I = 80 A, G = 25 slm, L = 80 mm)

enhanced radiation at the edge of the cathode end (gray value at the markers: 7 at 0.03 T and 28 at 0. 12 T). The more luminous cathode end indicated a rise in cathode temperature because the radiation of cathode was positively associated with the temperature in our experimental range. The temperature rise was possibly attributed to the reason that the heating power which was deposited on the cathode was enhanced in a larger magnetic field [34, 36]. It was inferred that the increase in cathode end temperature might increase the ability of the cathode to emit electrons [34, 39, 40], which may be one reason for the cathode spot expanding. Figure 7 reveals an explicit condition for the cathode spot rotating in the normal or reversed direction. The critical magnetic field, which reversed the movement direction of the cathode spot, was between 0.045 and 0.06 T. When the magnetic field was less than 0.045 T, the cathode spot moved in the normal direction, and the rotation speed decreased with an increase in the magnetic field. When the magnetic field was greater than 0.06 T, the cathode spot moved in the reversed direction. As the magnetic field increased, the rotation speed rose continuously, climbing from 6.2 r/min at 0.06 T to 24.8 r/min at 0.135 T.

Arc Current

Figure 8 shows the rotation speed and CCD images of the cathode spot under different arc currents. An increase in arc currents contributed to reversed movement of the cathode spot. The critical arc current for the reversal of the cathode spot was approximately 65 A when B = 0.06 T, G = 25 slm, and L = 80 mm in the argon atmosphere. The cathode spot also expanded rapidly with an increase in arc currents. The cathode spot diameter at 35 A was merely 2.7 mm; when the 125 A arc current was applied, the cathode spot diameter exceeded 5 mm. The brightness of the whole cathode end also increased in line with the

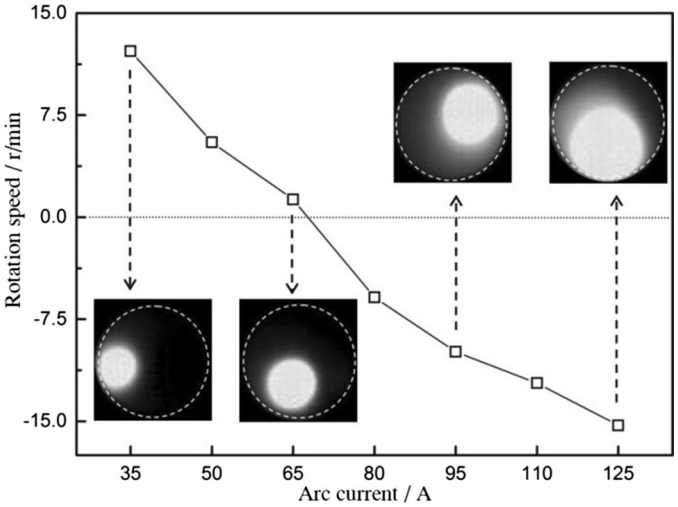

Fig. 8 Rotation speed and CCD images under different arc currents (B = 0.06 T, G = 25 slm, L = 80 mm, 0.5 μs shutter)

arc current. The expanding cathode spot and ascending temperature can be ascribed to the enhanced heating power which was deposited on the cathode under large arc currents.

Gas Flow

The rotation speed and CCD images of cathode spots under different levels of gas flow are presented in Fig. 9. Under a low flow rate (10 slm), the cathode spot had a large

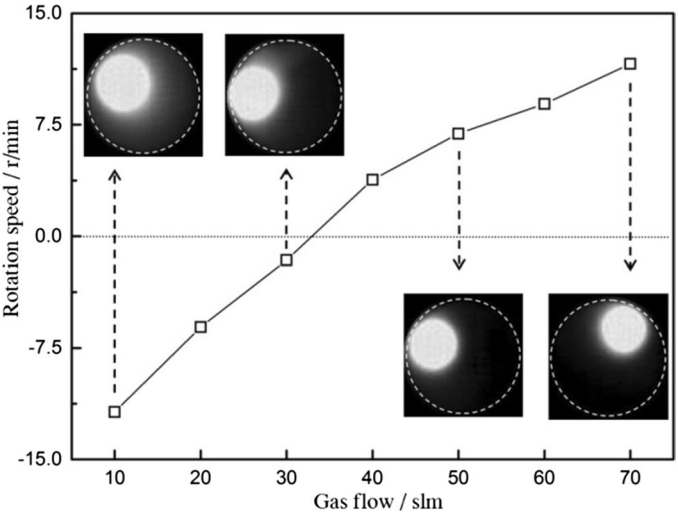

Fig. 9 Rotation speed and CCD images under different levels of gas flow (I = 80 A, B = 0.06 T, L = 80 mm, 0.5 μs shutter)

diameter (approximately 4 mm) and rotated in the reversed direction at a speed of 11.8 r/min. As the gas flow increased, the rotation speed of the cathode spot decreased and then the rotation direction reversed, moving in the normal direction when the gas flow exceeded 40 slm. Thus, an increase in gas flow contributed to normal movement of the cathode spot. Moreover, the cathode spot shrunk as gas flow increased, declining from 4 mm at 10 slm to 2.8 mm at 70 slm. Accordingly, the brightness of the whole cathode end declined, potentially due to the enhanced cooling effect of gas flow on the cathode.

Cathode Length

Figure 10 illustrates the effect of cathode length on cathode spot motion. In order to avoid the effect of magnetic field difference, the position of cathode end was approximately 50 mm in front of the anode exit by adjusting the moveable holder. Thus, the axial and radial component of magnetic field for different cathode rod lengths is basically the same near the cathode end. The cathode spot motion showed a similar evolution process under different cathode lengths. In a low magnetic field, the cathode spot moved in the normal direction. As the magnetic field increased, the rotation speed decreased, and then the spot moved in the reversed direction completely in a high magnetic field. However, the critical magnetic field for the reversal of the cathode spot movement was lower for a longer cathode. When L = 50 mm, the critical magnetic field was approximately 0.075 T; when L = 80 mm, the critical value was approximately 0.045 T. The critical value was only 0.03 T when L = 110 mm. CCD images in Fig. 10 reveal that the cathode spot expanded with an increase in cathode length, and a longer cathode presented a more luminous cathode end. Apparently, the weak cooling effect of the long cathode was possibly primarily responsible for an increase in cathode spot diameter and cathode end brightness.

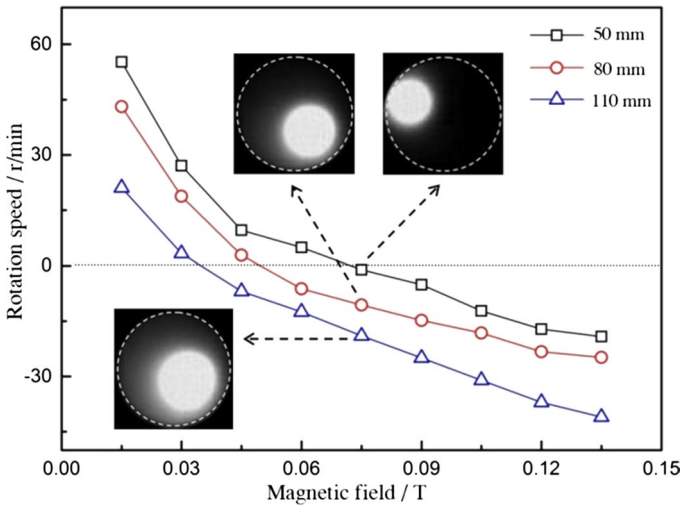

Fig. 10 Rotation speed and CCD images under different cathode lengths and different magnetic fields (I = 80 A, G = 25 slm, 0.5 μs shutter)

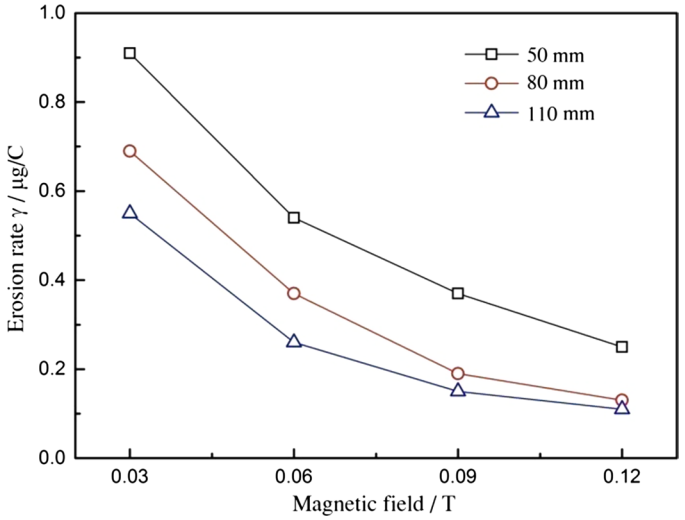

Fig. 11 Erosion rate measurements under different magnetic field and different cathode lengths (I = 80 A, G = 25 slm)

Erosion Rate of Cathode

Figure 11 shows the erosion rate measurements under different magnetic fields and different cathode lengths. Measurements of cathode erosion were obtained by comparing the initial and final weights of the graphite cathode for an arc operating for 30 min at a constant arc current and a constant gas flow. The result reveals the erosion rate of cathode decreased as the magnetic field increased but increased as the cathode length decreased. The erosion

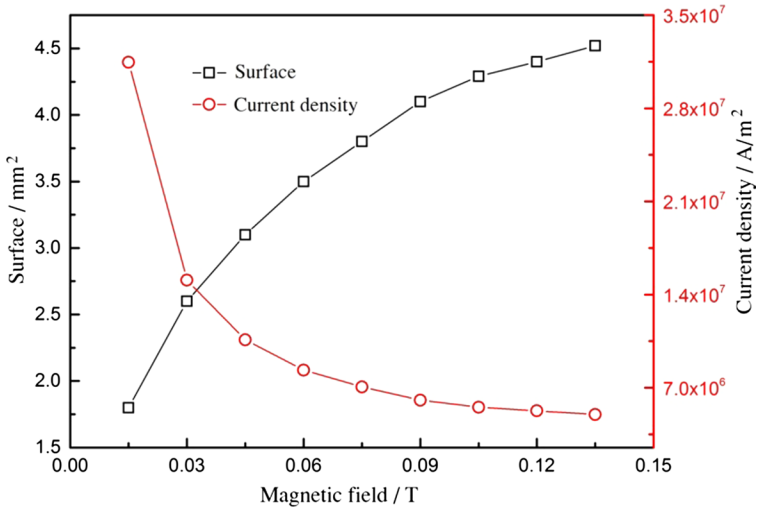

Fig. 12 Surface of cathode spot region and current density under different magnetic fields (I = 80 A, G = 25 slm, L = 80 mm)

rate was over 0.9 μg/C at a 0.03-T magnetic field and 50-mm cathode length but less than 0.2 μg/C at a 0.12-T magnetic field and 100-mm cathode length.

Figure 12 shows the measurements of the cathode spot region estimated from the CCD images obtained at various magnetic fields. The current density corresponding to the measurements in Fig. 12, calculated assuming a uniform current density within the cathode spot region, is also plotted in Fig. 12. The current density decreased with an increase in the magnetic field, declining from 3.1×10^7 A/m^2 at 0.015 T to 4.9×10^6 A/m^2 at 0.135 T; this result suggests that the average cathode surface temperature in the cathode spot decreased with an increase in the magnetic field. Due to the strong radiation emitted from the arc plasma in the cathode spot, the gray value in the CCD images was usually saturated in the cathode spot region. The images of the cathode end were obtained after the arc was extinguished for 0.2 ms. Given that the decay time of hot cathode radiation was more than 5 ms [41], the images after arc extinction for 0.2 ms truly reflect the cathode state during arc discharge. These images were processed using MATLAB software, so the gray value distribution on the cathode end was clearer as shown in Fig. 13. At 0.03 T, the gray value was distributed in a narrow region and the maximum value was 218 as shown in Fig. 13a. When the magnetic field reached 0.06 T and 0.09 T, the maximum gray value declined to 201 and 184, respectively, and increasing distribution regions appeared. The gray value was directly related to cathode temperature, revealing a similar temperature distribution. That is, for low magnetic fields, the peak temperature was high but the distribution region was small; for high magnetic fields, the cathode end had a wide high-temperature region but a low peak temperature.

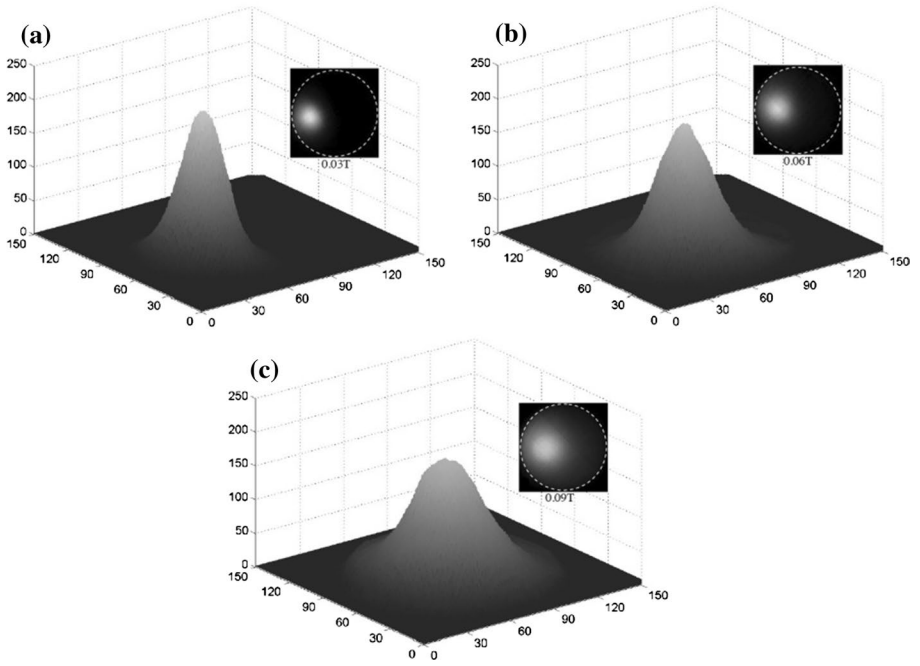

Fig. 13 Gray value distribution under different magnetic fields after arc extinction (I = 80 A, G = 25 slm, L = 80 mm, 0.5 μs shutter): **a** 0.03 T, **b** 0.06 T, **c** 0.09 T

As indicated above, the average current density (average temperature) and peak temperature in the cathode spot were lower in a high magnetic field, causing the erosion rate per unit area to decrease with an increase in the magnetic field. In the experimental range in Fig. 11, the erosion rate always decreased as the magnetic field increased. It is proposed that the decrease in erosion rate per unit area due to the decreasing average current density and peak temperature in the cathode spot outweighs the increase in the surface area of the cathode spot due to increasing magnetic field. This experimental result agrees with a study [42] in which the graphite cathode was operated in a specific current range. A similar analysis can explain the erosion rate difference under various cathode lengths; for the longer cathode, the weak cooling effect from the cathode bottom contributed to an expanding cathode spot as shown in Fig. 10. As a result, the low peak temperature of the cathode surface and low average current density in the cathode spot caused less erosion. In other words, the overcooling even can lead to a more severe erosion rate because of higher current density and higher peak temperature in the cathode spot.

Ignition Process

Based on the above findings, a reversal in cathode spot movement appeared to be related to several parameters, such as the magnetic field, arc current, gas flow, and cathode length. Further analysis confirmed that the normal movement of the cathode spot always corresponded to a cathode spot with a small area, whereas reversed movement corresponded to an expanding spot. In this section, the successive CCD images of the cathode end after ignition are presented. The arc operated at a constant magnetic field with a constant arc current, gas flow, and cathode length so the effect of cathode spot size on spot movement could be presented more clearly. Frames 1–8 in Fig. 14 depict the temporal and spatial evolution of the cathode spot after ignition. The rotation speed of the cathode spot and the arc voltages curves corresponding to Fig. 14 are plotted in Fig. 15. The rotation speed were obtained from successive images after 5 s of counting. Uncertainties in rotation speed were estimated to be around 50% because the rotation speed changed constantly. At 0.1 s, a luminous cathode spot with a small size (below 2 mm in diameter) emerged on the cathode end. The cathode end was so cold that the cathode outline could not be identified clearly.

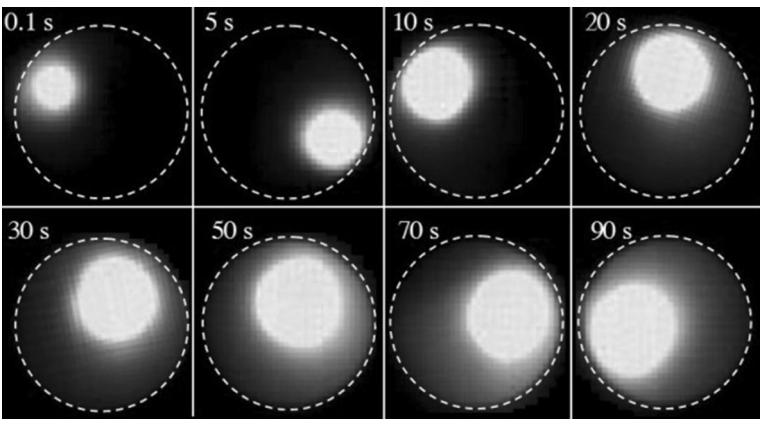

Fig. 14 Evolution of cathode spots versus time after ignition (I = 80 A, B = 0.075 T, G = 25 slm, L = 80 mm, 0.5 μs shutter)

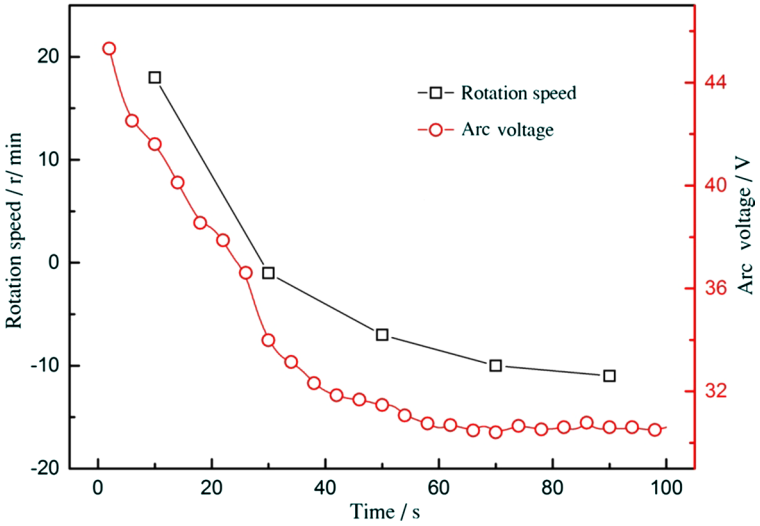

Fig. 15 Rotation speed of cathode spot and arc voltage corresponding to Fig. 14

As time went on, the cathode spot expanded gradually along with an increase in cathode end brightness. When the time exceeded 50 s, the cathode spot size and cathode end brightness did not change substantially. Figure 15 shows that the cathode spot moved in the normal direction in the first few seconds (approximately 30 s) and then reversed with an increase in discharge time. The rotation speed in the reversed direction increased with time until the rotation speed was fixed at approximately 10 r/min 60 s later. The evolution of cathode spot motion after ignition indicates that the reversal of the cathode spot movement seemed directly determined by the cathode spot size. Another interesting phenomenon is that, the arc voltage decreased as the discharge time increased, declining from 45.3 V at 0.1 s to 30.5 V at 60 s, after which the voltage maintained a stable value (approximately 30.5 V). For the argon rotating arc column, the voltage is less than 10 V/cm around 80 A [30]. In this paper, the cathode spot size changed after arc ignition, so the length of arc column changed accordingly. The length variation of the arc column was less than 5 mm, and the voltage change from the arc column should be less than 5 V. Figure 15 shows the voltage change was near 15 V, thus the cathode spot should play an important role in voltage variation.

Usually, the "cold-cathode" is referred to the "thermionic-field emissions" and the "hot-cathode" is referred to the "thermionic emission". In the thermal arc discharges, the electrode with low melting point, like copper cathode, has lower temperature that cannot provide enough "thermionic emission", so such electrode is called as cold-cathode. The electrode with high melting point (e.g. W) can have enough temperature to provide sufficient "thermionic emission", thus such electrode is called as hot-cathode. For graphite electrode, the graphite doesn't have a fixed melting point, and the electrode temperature is strongly affected by the cooling condition, thus the electrode may be "cold-cathode" or "hot-cathode", which has been reported by literature [43]. In this paper, the voltage curves indicate that the thermionic-field emission mechanism of the cathode may well play a more important role in initial arc discharge than in the later stage because of the colder cathode in the initial arc discharge.

Discussion

As shown in Fig. 16a, in the region near the cathode spot, the magnetic field B can be written as

$$\vec{B} = B_z\vec{z} + B_r\vec{r}$$

where r and z represent the radial component and axial component, respectively. Now, to be clear, the magnetic field shown in Fig. 2 does not exhibit the magnetic field direction; according to the current direction of magnetic coil, the B_r always points to the cathode center.

The arc current density J near the cathode spot can be read as

$$\vec{J} = J_z\vec{z} + \overrightarrow{J'}$$

where z represent the axial component. It's important to note that the direction of $\overrightarrow{J'}$ changes continually due to the arc rotation, as indicated in Fig. 3.

Hence, the Lorenz force can be written as

$$F_1 = J'B_z$$

$$F_2 = J_zB_r$$

F_1 is the driving force that impels the arc to rotate clockwise around the cathode (normal direction). Considering the fast and regular change of the $\overrightarrow{J'}$, F_1 should not have a major impact on the cathode spot movement. For example, the rotation cycle of cathode spot on the cathode end is about several seconds, whereas the arc has rotated for hundreds of cycles during this period driving by F_1. During the rotation cycle of cathode spot, the direction of F_1 changes all the time, thus the influence from F_1 is considered negligible. F_2 always points in the counterclockwise direction defined as the reversed motion as indicated in Fig. 16c. Clearly, the normal direction of the cathode spot movement thus actually opposes the Lorenz/Ampere direction which acts directly on the cathode spot. This phenomenon is similar to the retrograde movement that occurs in a vacuum/low-pressure arc with an external magnetic field. According to the latest experimental study and theoretical analysis, the retrograde movement of the cathode spot can be determined by the asymmetric magnetic pressure distribution around the

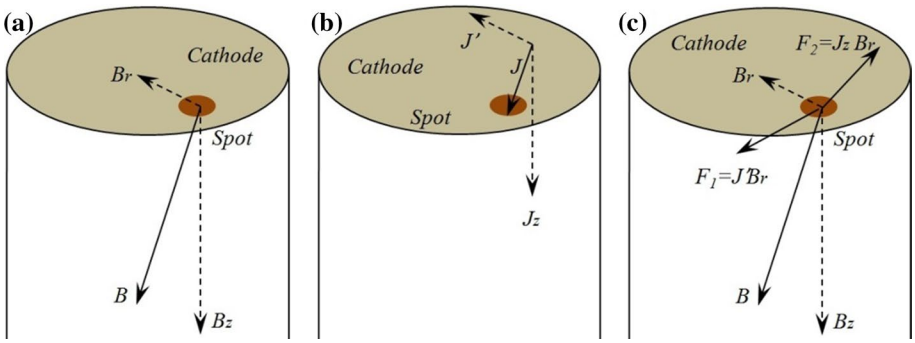

Fig. 16 Schematic diagram of the magnetic field, arc current and force analysis around the spot: **a** magnetic field, **b** arc current, **c** force analysis

spot [20, 23–25]. Driven by the pressure difference, the plasma configuration outside the spot becomes asymmetric, and the spot plasma contributes to jet ejection that helps to ignite new spots on the retrograde side. However, retrograde motion seems to be a feature of cold-cathode arcs exclusively, which are characterized by thermionic-field emissions. If the cathode is heated to a temperature high enough to support thermionic emissions, it is difficult to observe the retrograde motion of the cathode spot. In fact, for the hot graphite cathode, thermionic-field emissions can take place if the cathode is over-cooled, as indicated in Fig. 15 and the literature [43]; retrograde motion may occur in this situation. In this paper, the retrograde motion of the cathode spot may be explained by the magnetic pressure distribution.

As suggested by Beilis et al. [25], the magnetic pressure can be described as $\Delta P = 2B_r B_s/\mu$ as indicated in Fig. 16b. The B_s is the circular magnetic field which is induced by the arc current (J_z) in the cathode spot, and the B_s is basically positively associated with the current density (J_z) in the cathode spot. For the small cathode spot, the B_s is so strong that the pressure difference ΔP presents the potential for new spot ignition on the retrograde side. Thus, the cathode spot moves against the Ampere direction. With an increase in the cathode spot size, B_s decreases due to decreasing current density. As a result, the rotation speed of the cathode spot declines, and the movement direction is even reversed (Fig. 17).

To further confirm the existence of "magnetic pressure distribution" mentioned above, the effect of B_r on the cathode spot motion was presented here. The cathode end position was adjusted by moving the cathode holder. The location of the cathode end was 60, 50, 40, 30 and 20 mm in front of the anode exit, respectively. Because of the change of cathode end position, both the B_z and B_r around the cathode end changed. In this experiment, the current of magnetic coil was adjusted, so that the B_z was basically the same, thus the variation of cathode end position mainly reflected the difference of B_r. According to the results in Fig. 2, the B_r increased with the decrease of cathode end position when the B_z kept consistent.

Figure 18 shows the rotation speed and CCD images under different cathode end position with B = 0.06 T (B_z). Clearly, the size of cathode spot was similar under different cathode end position so the difference of B_s was negligible. For a higher B_r, the spot moved in the normal direction (retrograde direction); with the decrease of B_r (increase of cathode end position), the rotation speed declined, and the cathode spot can move in a reversed direction. This experimental phenomenon can qualitatively confirm the

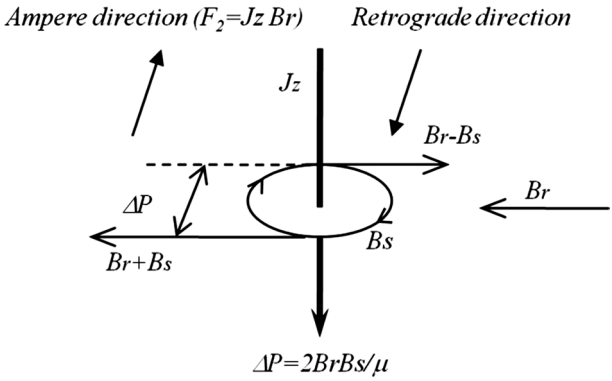

Fig. 17 Schematic diagram of the magnetic pressure difference near the cathode spot, *Bs*: self-magnetic field

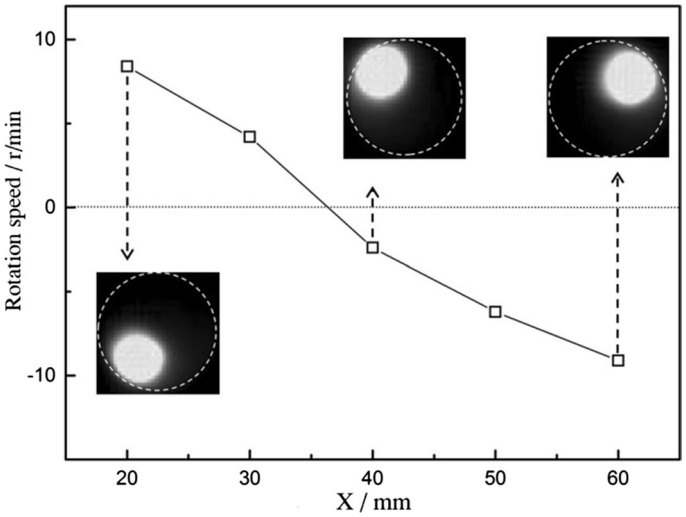

Fig. 18 Rotation speed and CCD images under different cathode end position (I = 80 A, B = 0.06 T, L = 80 mm, G = 25 slm, 0.5 μs shutter)

existence of "magnetic pressure distribution" because the pressure difference (ΔP) is proportional to the B_r($\Delta P = 2B_rB_s/\mu$).

The cathode spot observed in this work suggests that cathode spot velocity and its reversal depend on the magnetic field, arc current, gas flow, and cathode rod length. Based on the magnetic pressure difference theory, the cathode spot motions may be explained by the current density difference in the cathode spot. For various arc currents, the region of the cathode spot increased with an increase in the arc current, and the average current density presented a declining trend within the experimental range, so reversed motion occurred at a higher arc current. For various cathode rod length, the region of cathode spot is larger for long cathode rod, thus the reversed motion is favored by the long cathode rod. For different magnetic fields, the difference in cathode spot motion can be attributed to a decrease in B_s due to decreasing current density in the cathode spot, which possibly outweighs the increase in B_r due to the increasing magnetic field.

Conclusion

In this study, cathode spot motion in a magnetically rotating arc plasma generator is experimentally researched at atmospheric pressure. The configuration of the cathode spot on a graphite cathode is observed at different magnetic fields, arc currents, gas flow and cathode lengths. The main conclusions are as follows:

1. The cathode spot rotates on the cathode end at a low speed (less than 1 Hz). For a low magnetic field, low arc current, high gas flow, or short cathode rod, the rotation direction of the cathode spot is consistent with that of the arc column (called the normal direction). With an increase in the magnetic field, increase in arc current, decrease in gas flow, or increase in the cathode rod length, the rotation speed declines, and the cathode spot

can move in the reversed direction. The critical condition for reversed motion relates to the magnetic field, arc current, gas flow, and cathode length.

2. When the spot motion transfers from the normal direction to the reversed one, the cathode spot area expands gradually. Expansion in the cathode spot region may result from better heating on the cathode end. Due to the expanding cathode spot, both the average current density and peak temperature of the cathode spot decrease, and the cathode erosion rate declines.
3. Further analysis indicates that the normal motion of the cathode spot actually opposes the Lorenz/Ampere direction induced by the radial component of the magnetic field. The cathode spot motion (normal direction) is similar to the retrograde movement that occurs in the vacuum arc with an external magnetic field. Considering that the thermionic-field emission mechanism of the cathode may exist in the hot graphite cathode, the magnetic pressure difference is used to explain the cathode spot motion. The spot motion may be primarily due to the current density in the cathode spot, which directly affects the self-magnetic field. Thus, the cathode spot with a small region would tend to move against the Lorenz/Ampere direction because of a higher magnetic pressure difference.

Acknowledgements The work is supported by National Natural Science Foundation of China (No. 11705202) and Anhui Provincial Natural Science Foundation (No. 1808085MA12).

References

1. Fauchais P, Vardelle A (1997) Thermal plasmas. IEEE Trans Plasma Sci 25:1258–1280
2. Pfender E (1999) Thermal plasma technology: where do we stand and where are we going? Plasma Chem Plasma Process 19:1–31
3. Slinkman D, Sacks R (1990) Structure and dynamics of a magnetron DC arc plasma. Appl Spectrosc 44:76–83
4. Xia WD, Li LC, Zhao YH, Ma Q, Du BH, Chen Q, Cheng L (2006) Dynamics of large-scale magnetically rotating arc plasmas. Appl Phys Lett 88:211501
5. Wang C, Li WW, Zhang XN, Zha J, Xia WD (2015) Evolution of magnetically rotating arc into large area arc plasma. Chin Phys B 24:065206
6. Szente RN, Munz RJ, Drouet MG (1987) The effect of low concentrations of a polyatomic-gas in argon on erosion on copper cathodes in a magnetically rotated arc. Plasma Chem Plasma Process 7:349–364
7. Szente RN, Munz RJ, Drouet MG (1987) Effect of the arc velocity on the cathode erosion rate in argon nitrogen mixtures. J Phys D Appl Phys 20:754–756
8. Szente RN, Munz RJ, Drouet MG (1988) arc velocity and cathode erosion rate in a magnetically driven arc burning in nitrogen. J Phys D Appl Phys 21:909–913
9. Pan WX, Lu FX, Tang WZ, Zhong GF, Jiang Z, Wu CK (2000) Carbon transition efficiency and process cost in high-rate, large-area deposition of diamond films by DC arc plasma jet. Diam Relat Mater 9:1682–1686
10. Lu FX, Tang WZ, Huang TB, Liu JM, Song JH, Yu WX, Tong YM (2001) Large area high quality diamond film deposition by high power DC arc plasma jet operating at gas recycling mode. Diam Relat Mater 10:1551–1558
11. Ma J, Zhang M, Wu J, Yang Q, Wen G, Su B, Ren Q (2017) Hydropyrolysis of n-hexane and toluene to acetylene in rotating-arc plasma. Energies 10:899
12. Zhang M, Xue W, Su B, Bao Z, Wen G, Xing H, Ren Q (2017) Conversion of glycerol into syngas by rotating DC arc plasma. Energy 123:1–8
13. Slinkman D, Sacks R (1990) A magnetron DC arc plasma for aerosol analysis. Appl Spectrosc 44:83–90
14. Mihovsky MK, Hadzhiyski V (2009) Transport and heat phenomena of transferred DC arc under auto-electro-magnetic rotation (AEMR) in plasmalab reactor. High Temp Mater Process (New York) 13:121–135

15. Hadzhiyski V, Mihovsky M, Gavrilova R (2011) Plasma-arc reactor for production possibility of powdered nano-size materials. J Phys Conf Ser 275:012005
16. Carter RP, Murphree DL (1969) Low-pressure arc discharge motion between concentric cylindrical electrodes in a transverse magnetic field. AIAA J 7:1430
17. Hernqvist KG, Johnson EO (1955) Retrograde motion in gas discharge plasmas. Phys Rev 98:1576–1583
18. Murphree DL, Carter RP (1970) Photographic observations of the retrograde rotation of an arc discharge. Phys Fluids 13:1747–1750
19. Drouet MG (1981) The physics of the retrograde motion of the electric arc. IEEE Trans Plasma Sci 13:235–241
20. Drouet M, Meunier JL (1985) Influence of the background gas pressure on the expansion of the arc-cathode plasma. IEEE Trans Plasma Sci 13:285–287
21. Schrade HO (1989) Arc cathode spots: their mechanism and motion. IEEE Trans Plasma Sci 17:635–637
22. Moizhes BY, Nemchinsky V (1991) On the theory of the retrograde motion of a vacuum arc. J Phys D Appl Phys 24:2014
23. Juttner B (2001) Cathode spots of electric arcs. J Phys D Appl Phys 34:R103
24. Juttner B, Kleberg I (2000) The retrograde motion of arc cathode spots in vacuum. J Phys D Appl Phys 33:2025
25. Beilis II (2002) Vacuum arc cathode spot grouping and motion in magnetic fields. IEEE Trans Plasma Sci 30:2124–2132
26. Schrade HO (2002) Arc cathode spots: their mechanism and motion. IEEE Trans Plasma Sci 17:635–637
27. Bobrov YK, Bystrov V, Rukhadze A (2006) Physical model of the cathode spot retrograde motion. Tech Phys 51:567–573
28. Szente RN, Munz RJ, Drouet MG (1990) The influence of the cathode surface on the movement of magnetically driven electric-arcs. J Phys D Appl Phys 23:1193–1200
29. Wang C, Cui HC, Zhang ZL, Xia WL, Xia WD (2017) Observation of arc modes in a magnetically rotating arc plasma generator. Contrib Plasma Phys 57:395–403
30. Chen T, Wang C, Liao MR, Xia WD (2016) Diffuse and spot mode of cathode arc attachments in an atmospheric magnetically rotating argon arc. J Phys D Appl Phys 49:085202
31. Chen T, Li H, Bai B, Liao MR, Xia WD (2016) Parametric study on arc behavior of magnetically diffused arc. Plasma Sci Technol 18:6–11
32. Chen T, Wang C, Zhang XN, Zhang H, Xia WD (2017) Thermal and electrical influences from bulk plasma in cathode heating modeling. Plasma Sources Sci Technol 26:025002
33. Bai B, Zha J, Zhang XM, Wang C, Xia WD (2012) Simulation of magnetically dispersed arc plasma. Plasma Sci Technol 14:118–121
34. Wang C, Zha J, Li WW, Xia WL, Xia WD (2014) Experimental study of the thermal cathodic arc root in magnetically rotating arc plasma. High Volt Eng 40(10):3025–3031
35. Xia WD, Zhou HL, Zhou ZP, Bai B (2008) Evolution of cathodic arc roots in a large-scale magnetically rotating arc plasma. IEEE Trans Plasma Sci 36:1048–1049
36. Wang C, Li WW, Zhang XN, Liao MR, Zha J, Xia WD (2015) Observation of thermal cathodic hot spots in a magnetically rotating arc plasma generator. IEEE Trans Plasma Sci 43:3716–3720
37. Mihovsky MK, Hadzhiyski V, Todorov L (2007) Electromagnetic and gas dynamic control of transferred plasma ARC in metallurgical plasma reactors and furnaces. High Temp Mater Process (New York) 11:359–369
38. Zhou HL, Li LC, Cheng L, Zhou ZP, Bai B, Xia WD (2008) ICCD imaging of coexisting arc roots and arc column in a large-area dispersed arc-plasma source. IEEE Trans Plasma Sci 36:1084–1085
39. Dabringhausen L, Nandelstadt D, Luhmann J, Mentel J (2002) Determination of HID electrode falls in a model lamp I: pyrometric measurements. J Phys D Appl Phys 35:1621–1630
40. Lichtenberg S, Nandelstadt D, Dabringhausen L, Redwitz M, Luhmann J, Mentel J (2002) Observation of different modes of cathodic arc attachment to HID electrodes in a model lamp. J Phys D Appl Phys 35:1648–1656
41. Haidar J, Farmer A (1993) A method for the measurement of the cathode surface temperature for a high-current free-burning arc. Rev Sci Instrum 64:542–547
42. Haidar J (1996) An experimental investigation of high-current arcs in argon with graphite electrodes. Plasma Sources Sci Technol 5:748–753
43. Seon H, Munz RJ (2001) Study of arc stability and erosion behaviour of a transferred arc with graphite DC electrodes. Can J Chem Eng 79:626–632